Long-wavelength Pol-InSAR for glacier ice extinction estimation

Jayanti J. Sharma, Irena Hajnsek*, Konstantinos P. Papathanassiou
Microwaves and Radar Institute, German Aerospace Center (DLR), Münchner Straße 20, 82234 Weßling, Germany
*DLR and Institute of Environmental Engineering, ETH Zürich, Wolfgang-Pauli-Str. 15, CH-8093 Zurich, Switzerland
Email: jayanti.sharma@dlr.de, irena.hajnsek@dlr.de, kostas.papathanassiou@dlr.de

Abstract

In recent years there has been increased interest in using synthetic aperture radar (SAR) to study and monitor glaciers for climate change research. This paper describes the estimation of ice extinctions through modelling of Pol-InSAR (polarimetric interferometric SAR) coherences as a combination of a surface contribution (from the snow-firn interface and wind-induced features) and a volume response. Ground-to-volume scattering ratios derived from a novel polarimetric decomposition are used in conjunction with Pol-InSAR interferometric coherence magnitudes to invert the extinction of the ice layer. The inversion is performed with experimental airborne Pol-InSAR data at L- and P-band collected using DLR's E-SAR system over the Austfonna ice cap in Svalbard, Norway as part of the 2007 ICESAR campaign. Extinction-dependencies on frequency and glacier zone are investigated, and validation is performed comparing P-band sounder data to inverted extinction values.

1 Introduction

In the last decade Pol-InSAR has become an established technique for the extraction of geophysical parameters from volume scatterers, particularly for vegetation applications. However, the use of Pol-InSAR over glaciers to date is restricted to a small number of airborne studies [1,2] due to limited data availability and to difficulties in validation.

The goal of this work is to develop and invert a model parameterising Pol-InSAR observables in terms of glacial properties. A model relating interferometric coherence and extinction is proposed which takes into account the influence of both volume and surface scattering. Extinction is a relevant parameter for glaciologists as it contains information on the density and internal structure of the ice.

The extinction modelling approach is presented in section 2. Experimental Pol-InSAR data collected at L- and P-band using DLR's E-SAR system are described in section 3 and are used in section 4 to invert extinctions for the Austfonna ice cap in Svalbard, Norway. Results are validated against extinctions derived from nadir-looking P-band sounder data. A summary of the results is given in section 5.

2 Modelling glacier ice extinctions

Extinction accounts for the combined effects of absorption and scattering in a medium and may be expressed as $\kappa_e = \cos\theta_r / d_{\text{pen}}$ where d_{pen} is the penetration depth at which the one-way power falls to $1/e$. The $\cos\theta_r$ factor accounts for the off-vertical travel distance of the wave within the medium and θ_r is the incidence angle after refraction. κ_e is the one-way power extinction coefficient in units of Nepers/m, although it is conventionally quoted in decibels as $10\log_{10} e^{\kappa_e}$ dB/m.

A simple model relating extinction and interferometric coherence is proposed which is based on the work of [2, 3] and is extended through parameterisation of the relative surface and volume contributions by means of polarimetric decomposition (section 2.1). This permits a new closed-form solution for extinction (section 2.2).

2.1 Ground-to-volume scattering ratios

The radar signal is a superposition of all scattering contributions in the illuminated scene, and surface and volume components must be separated in order to determine geophysical properties of the ice volume. A 3-component polarimetric decomposition for glacier ice is used, consisting of a ground component from the snow-firn interface (described by the first-order Small Perturbation Method (SPM)), a random volume of dipoles and an oriented sastrugi field (caused by wind-induced features at the snow surface). Assuming components are uncorrelated, the combined covariance matrix is a sum of the matrices for the individual mechanisms:

$$[C_{\text{total}}] = [C_g] + [C_v] + [C_s], \tag{1}$$

where subscript g is ground (i.e. snow-firn interface), v is volume and s is sastrugi. Covariance matrices for each component are given in [4] .

The ground-to-volume scattering ratio m is defined to quantify the relative surface and volume power contributions for each polarisation in the H-V basis. m is computed using the powers along the main diagonals of the modelled covariance matrices:

$$\begin{aligned} m_{\text{HH}} &= \frac{C_{g\,11} + C_{s\,11}}{C_{v\,11}} \\ m_{\text{HV}} &= \frac{C_{s\,22}}{C_{v\,22}} \\ m_{\text{VV}} &= \frac{C_{g\,33} + C_{s\,33}}{C_{v\,33}}. \end{aligned} \tag{2}$$

Note that a ground contribution for HV ($C_{g\,22}$) is not included in Eq. 2 because the first-order SPM does not predict a cross-polar component.

2.2 Coherence model for glacier ice

The ground-to-volume scattering ratios are used in combination with Pol-InSAR coherences for determination of the ice extinction coefficient. The ice volume is assumed to consist of material in an intermediate stage between snow and pure ice called *firn*. The firn volume is modelled as a semi-infinite half-space consisting of a uniform distribution of scatterers with relative dielectric constant $\varepsilon_r \simeq 2.8$. The firn volume extends from the snow-firn surface (located at $z = 0$) downwards with radar viewing geometry given in **Figure 1**. The two antennae are separated by baseline B and observe a point on the ground at incidence angle θ. As the EM wave enters the snow, it is refracted at an angle θ_{snow} to the vertical, and is refracted once more to θ_r in the ice volume according to Snell's law. The difference in look angles from each antenna is $\Delta\theta$ in air and $\Delta\theta_r$ in the volume (not shown).

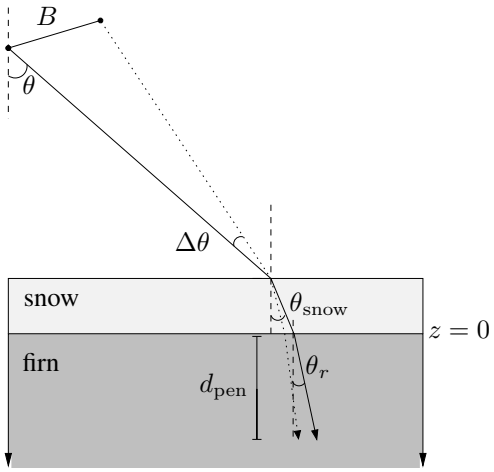

Figure 1: InSAR geometry (not to scale) for a glacier scenario assuming an infinite uniform volume.

The principle Pol-InSAR observable is the complex coherence γ. Neglecting temporal decorrelation and assuming sufficient compensation of system (e.g. Signal-to-Noise Ratio) and geometric (range spectral shift) decorrelation contributions, γ is dependent solely on the vertical distribution of scatterers. The coherence magnitude $|\gamma|$ is postulated to be a combination of volume scattering with complex coherence γ_{vol} and a surface scattering component whose relative strength is given by ground-to-volume scattering ratio m [2]:

$$|\gamma| = \left| \frac{\gamma_{\text{vol}}(\kappa_e) + m}{1 + m} \right|, \tag{3}$$

where, due to an unknown snow depth, it is assumed that sastrugi and ground contributions both lie at $z = 0$. Assuming an infinite, uniform volume, γ_{vol} can be represented by [5]:

$$\gamma_{\text{vol}} = \frac{1}{1 + \frac{j \cos\theta_r k_{z\text{vol}}}{2\kappa_e}}, \tag{4}$$

where $k_{z\text{vol}} = \frac{4\pi\sqrt{\varepsilon_r}}{\lambda} \frac{\Delta\theta_r}{\sin\theta_r}$ is the vertical wavenumber in the volume, j is the imaginary unit, and λ is the wavelength in free space. Multiple scattering is neglected and it is assumed that topographic variations are negligible, which is reasonable for the relatively flat ice caps and sheets examined here.

With knowledge of m from Eq. 2, κ_e can be determined using Eqs. 3 and 4 at each polarisation and each pixel independently:

$$\kappa_e = \frac{\cos(\theta_r)|k_{z\text{vol}}|}{2(1+m)} \sqrt{\frac{|\gamma|^2(1+m)^2 - m^2}{1 - |\gamma|^2}}. \tag{5}$$

The absolute value $|k_{z\text{vol}}|$ is taken to obtain a positive (and physically meaningful) extinction when selecting the positive square root in Eq. 5.

3 Experimental data

The test sites are located on the Austfonna ice cap, situated in Svalbard, Norway (79.7°N, 24.0°E). Two sites were overflown, one in the firn zone near the summit of the ice cap (referred to as 'Summit'), and one in the superimposed ice (SI) zone near the Etonbreen outlet glacier ('Eton'). The firn zone is characterised by percolation features caused by refrozen meltwater whereas the SI zone consists of more homogeneous ice. Topography is very gentle with surface slopes of less than 1° at both sites.

Airborne SAR data were acquired over the test sites as part of the ICESAR campaign in spring 2007, which was a joint project between the Microwaves and Radar Systems Institute of the German Aerospace Center (DLR) and the Alfred-Wegener Institute, and supported by the European Space Agency (ESA). Repeat-pass fully-polarised L-band (1.3 GHz) and P-band (350 MHz) data were collected using DLR's E-SAR system as well as single-pass nadir-looking P-band sounder data (also at 350 MHz).

4 Results and Discussion

4.1 Extinction inversion

Polarimetric decomposition as described in section 2.1 was applied on a pixel-by-pixel basis to the experimental data. Ground-to-volume scattering ratios estimated from Eq. 2 were then used in combination with Pol-InSAR coherences in Eq. 5 for determination of the ice extinction coefficient. Detailed decomposition results are presented in [4], and thus the focus in this study is on the extinctions and their validation. A spatial averaging window of 100 effective looks was used to compute interferometric coherences. Results from multiple baselines (up to six) were combined by first applying a mask of $0.01 < k_z < 0.1$ to eliminate solutions from extremely small baselines (which have virtually no interferometric sensitivity) and from longer baselines more susceptible to insufficiencies in modelling and to uncertainties in m and $|\gamma|$. Results were then averaged from the remaining valid baselines on a pixel-by-pixel basis.

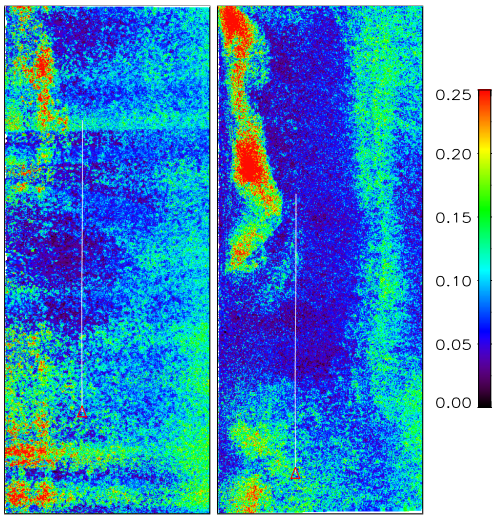

Figure 2: Extinctions κ_e [dB/m] at HH for Summit L-band (left) and P-band (right). Location of P-band sounder profiles are shown in white, where the red triangle indicates the start position of the profile.

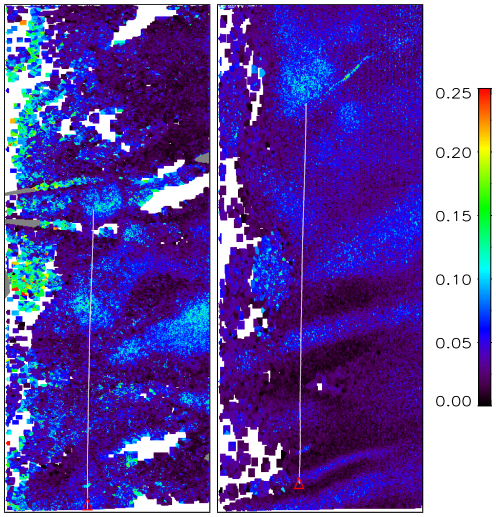

Figure 3: Same as **Figure 2** for Eton L-band (left) and P-band (right).

Table 1: Mean extinctions averaged across the entire image (Pol-InSAR) and across the sounder profile.

		mean κ_e [dB/m]			
		HH	**VV**	**HV**	**Sounder HV**
Summit	L	0.103	0.131	0.117	
	P	0.094	0.091	0.125	0.087
Eton	L	0.047	0.064	0.079	
	P	0.040	0.033	0.107	0.057

Inverted extinction coefficients at HH polarisation for L- and P-band at both Summit and Etonbreen test sites are given in **Figures 2** and **3**. Pixels for which none of the baselines satisfied the k_z criteria are shown in gray and pixels in white could not be inverted. Extinctions averaged over each image are shown in **Table 1** to compare results between test sites, frequencies and polarisations.

As expected, extinctions at Etonbreen are lower than those at Summit due to the lack of large-scale melt features to produce volume scattering. Some areas of Etonbreen could not be inverted because the square root in Eq. 5 becomes negative due to a large m which is inconsistent with the measured decorrelation $|\gamma|$. For the co-pols, L-band shows slightly higher extinctions than P-band (**Table 1**), which is expected from scattering theory that predicts both absorption and scattering extinction coefficients to increase with increasing frequency.

The P-band cross-pol shows elevated extinction values at both test sites which are attributed to the presence of an uncompensated ground component. This is possible as the first-order SPM used in this study for surface scattering predicts an HV contribution of zero, and thus second-order terms from the SPM or an alternate model should perhaps be considered for low-frequency surface scattering such as from P-band. However, the similarity of the co-pol extinctions at P-band and all polarisations at L-band suggests that the random volume assumption of the model (predicting polarisation-independent κ_e) is reasonable.

Deviations from a random volume however will result in inaccuracies in modelled m and κ_e. To permit inversion, the observation space could be extended using a unified polarimetric and interferometric approach (instead of being applied in two steps as done here) utilizing both amplitude and phase information, although the challenge remains of finding a model consistent with all observables.

4.2 Validation with Sounder data

Validation of inverted extinctions is carried out using P-band sounder data acquired nearly simultaneously to the Pol-InSAR data, where sounder profile locations are shown in **Figures 2** and **3**. The received power versus depth (z) recorded by the sounder was converted to a weighted relative scattering cross section σ_w using the radar equation by:

$$\sigma_w(z) = \frac{P_r(z)R^2(z)}{V_s(z)}C, \tag{6}$$

where P_r is the received power, R the range, V_s is the scattering volume at this range bin and C is a constant factor including transmit power, wavelength and antenna gain terms. There is an R^2 dependence in Eq. 6 rather than R^4 after [6], since for a planar interface such as a smooth ice layer, considerably more backscattered energy is returned to a nadir-looking receiver. σ_w is related to extinction through $\sigma_w = \sigma_v e^{-2\kappa_e R}$, where σ_v is the volume scattering cross section. No absolute characterisation of σ_v is possible due a lack of radiometric calibration. σ_w is

normalised such that $\sigma_{w\,\mathrm{norm}} = 0$ dB at $z = 0$ for HH, and a linear fit of $\ln \sigma_{w\,\mathrm{norm}}(z)$ versus depth yields an estimate of the power extinction rate κ_e. **Figure 4** shows $\sigma_{w\,\mathrm{norm}}$ versus depth for the Summit test site averaged across the entire sounder profile. The co-pols HH and VV are corrupted by strong off-nadir surface clutter interference, although HV shows a nearly constant extinction rate with increasing depth, confirming the uniform ice volume model assumption in section 2.2.

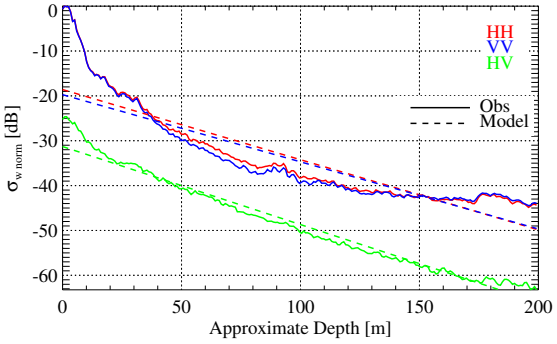

Figure 4: Normalised σ_w [dB] versus depth for P-band sounder data (averaged over the entire profile) overplotted with linear fit.

Fitted κ_e values at HV for the sounder data are given in **Table 1**. Extinction results compare favourably to inverted P-band values from Pol-InSAR. Slightly higher extinctions for the sounder data compared to the Pol-InSAR co-pols at Eton could be due to englacial layer-type scattering which in the model was assumed to come from the surface at $z = 0$ and removed during polarimetric decomposition. κ_e from Pol-InSAR thus reflects only volume-type scattering and leads to reduced overall extinction estimates.

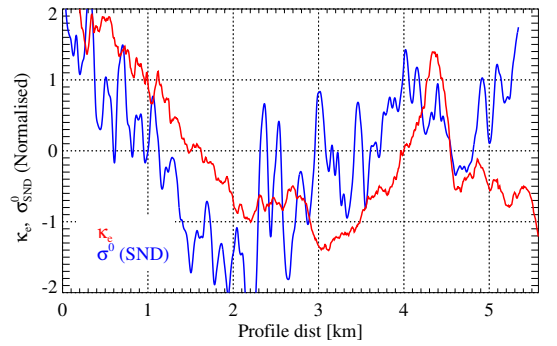

Figure 5: Normalised P-band κ_e HH (red) and P-band HV sounder σ^0_{SND} (blue) profiles for Summit.

To determine whether changes in subsurface scattering over the sounder profile are correlated with changes in extinctions inverted with Pol-InSAR, σ_w values are transformed into an equivalent sounder backscattering coefficient σ^0_{SND} through integration over depth. The sounder backscattering coefficients are scaled to zero mean and unity standard deviation for comparison with the inverted extinctions. **Figure 5** plots scaled and normalised κ_e and σ^0_{SND} coefficients for P-band at the Summit test site. There is a clear correlation between sounder subsurface backscatter and inverted extinctions from Pol-InSAR, implying that both systems are observing the same ice structure.

5 Summary

In this paper a model relating Pol-InSAR observables to glacier ice extinctions has been presented and inverted for experimental airborne data at L- and P-band. The modelling approach was divided into two parts: ground-to-volume scattering ratios were derived through polarimetric decomposition into volume, surface and sastrugi components. These ratios were then used in conjunction with Pol-InSAR coherences and an infinite, uniform-volume-underground model to invert ice extinctions. Inverted extinctions compare favourably with P-band sounder subsurface extinction rates and with changes in subsurface sounder backscatter across the profile.

The presented extinction model may be useful for examining the long-term variability of polar regions by tracking interannual changes in extinction. Future spaceborne concepts such as the BIOMASS Earth observation proposal (P-band) would also benefit from an increased understanding of long-wavelength radar observables over glacier ice.

Acknowledgments

The authors extend their thanks to Dr. Rolf Scheiber for his processing of the P-band sounder data. This work has been funded by DLR and the data collection was supported by ESA under contract 20655/07/NL/CB.

References

[1] O. Stebler, A. Schwerzmann, M. Lüthi, E. Meier, and D. Nüesch, "Pol-InSAR observation from an alpine glacier in the cold infiltration zone at L- and P- band," *IEEE Geosci. Remote Sens. Lett.*, vol. 59, pp. 357–361, July 2005.

[2] J. Dall, K. P. Papathanassiou, and H. Skriver, "Polarimetric SAR interferometry applied to land ice: modeling," in *Proc. of the European Conference on Synthetic Aperture Radar (EUSAR)*, Ulm, Germany, May 2004, pp. 247–250.

[3] E. W. Hoen and H. Zebker, "Penetration depths inferred from interferometric volume decorrelation observed over the Greenland ice sheet," *IEEE Trans. Geosci. Remote Sens.*, vol. 38, no. 6, pp. 2572–2583, November 2000.

[4] J. J. Sharma, I. Hajnsek, K. P. Papathanassiou, and A. Moreira, "Polarimetric decomposition over glacier ice with long-wavelength Pol-SAR (submitted)," *IEEE Trans. Geosci. Remote Sens.*

[5] J. J. Sharma, I. Hajnsek, and K. P. Papathanassiou, "Multi-frequency Pol-InSAR signatures of a subpolar glacier," in *3rd Intl. Workshop on Sci. and Appl. of SAR Polarimetry and Polarimetric Interferometry (PolInSAR)*, Frascati, Italy, 22-26 January 2007.

[6] D. Daniels, Ed., *Ground Penetrating Radar*, 2nd ed. London, Institution of Electrical Engineers, IEE Radar, Sonar and Navigation and avionics Series 15, 2004.